Chapter 4

Transcriptome analysis of CD8 T cells to inform a targeted CRISPR screen

4.1 Introduction

TCR stimulation triggers naive CD8 T cells to differentiate into effector CTL. This causes a small and quiescent naive cell to undergo rapid clonal expansion, substantially increase in size and acquire effector functions (de la Roche et al., 2016). The genome will be identical between a naive CD8 T cell and its corresponding differentiated effector CTL version, but the genes that are actively expressed will likely differ. In this chapter, RNA-seq was used to understand what genes are differentially expressed between naive and effector CD8 T cells. RNA-seq allows measurement of the complete set of transcripts of a cell (Wang et al., 2009) and therefore allowed me to determine which genes are upregulated in response to activation. Some of these upregulated genes will be necessary for CTL effector functions, such as target cell killing. The result of this RNA-seq project formed the basis of a subsequent screen to investigate how CD8 T cells are regulated at the genetic level. Targeting hits from the RNA-seq dataset using the CRISPR technology, as optimised in chapter 3, allowed me to determine whether the upregulated genes affect CTL killing function.

4.1.1 Study design

The experimental approach was to compare the transcriptome of naive CD8 T cells freshly isolated from spleens of WT mice ("day 0" samples) to the transcriptome of effector CD8 T cells that were activated on αCD3ε and αCD28 antibody-coated plates for two days, followed by 5 days of expansion ("day 7" samples) (Figure 4.1A). This experimental design

was identical to the standard procedure used to activate WT mouse T cells in vitro. Day 7 was chosen as the end time point as cells are typically used for functional assays, such as degranulation or killing assays, around this time. At the time that the RNA-seq experiment was performed the plan was to use T cells derived from Cas9 hom mice for the screen. As the Cas9 hom mice were on a C57BL/6 background, WT C57BL/6 mice were used for the RNA-seq study. The study included cells from 10 different mice (4 males and 6 females, all $\sim$16 weeks old). While the main question of interest was what genes are differentially expressed in day 7 vs day 0 samples, the RNA-seq dataset could additionally be used to investigate differentially expressed genes between males and females.

4.1.2 Chapter aims

- Determine the differences in gene expression between naive and activated CD8 T cells. The hypothesis is that there are substantial changes in gene expression between these two states of CD8 T cells.
- Explore the functional association of the differentially expressed genes using bioinformatic tools.
- Test the effect of targeting differentially expressed genes by CRISPR in phenotypic assays (degranulation and killing assays).
- Explore what genes are differentially expressed in CD8 T cells derived from male and female mice.

4.2 Results

4.2.1 RNA sample preparation and quality control

CD8 T cells were purified from spleens derived from WT mice to ensure that the RNA-seq data was predominantly derived from CD8 T cells. In order to have a record of the CD8 purity of each sample, the percentage of CD8 positive cells was determined by flow cytometry on the same day as freezing cell pellets for RNA extraction. CD8 positive cells constituted >94.7% of all samples except for one sample where the percentage of CD8s was slightly lower (Sample 33 day 7: 87.5%) (Figure 4.1B). After RNA extraction with the RNeasy Mini Kit (Qiagen), the quality of RNA was tested using a Bioanalyser (Agilent). High quality RNA is critical to ensure successful library preparation for sequencing. The Bioanalyser determined RNA quality by estimating a RNA integrity number (RIN) (Schroeder

et al., 2006). The Bioanalyser electrophoretically separated RNA fragments and visualised their size and distribution via laser-induced fluorescence (see Figure 4.1C and D for a representative bioanalyser gel and electrophoretic trace). The RIN algorithm takes the entire electrophoretic trace into account before allocating a score between 1 and 10 to the sample, with 10 indicating highest quality RNA (Schroeder et al., 2006). Library preparation and sequencing was performed by the Illumina bespoke team at the Sanger Institute. For library preparation the Illumina bespoke team required the RNA samples to have a RIN value higher than 8. All RNA samples in this study had a RIN score between 8.2 and 9.6 (Figure 4.1E). The Illumina bespoke team performed a stranded library prep with oligodT pulldown. The 20 samples (10 samples for day 0 and 10 samples for day 7) were pooled across 3 paired-end lanes of an Illumina Hi-Seq and 75 bp reads were sequenced.

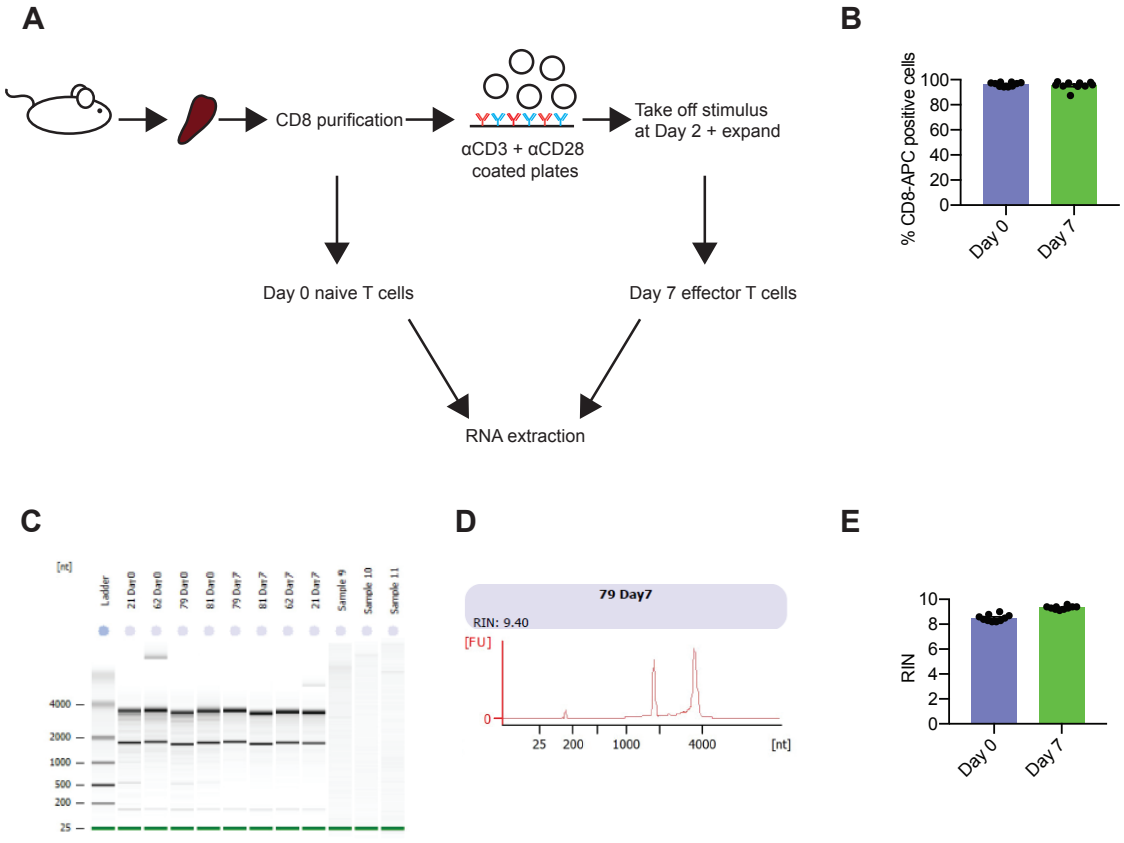

Fig. 4.1 ***RNA-seq study design and sample preparation.***

Fig. 4.1 ***RNA-seq study design and sample preparation.*** ***A*** *CD8 T cells were purified from spleens derived from C57BL/6N WT mice (10 biological replicates, 4 males and 6 females) across two spleen collection dates. After purification, 6 million cells per sample were frozen as "day 0" naive cells. The remaining cells were stimulated for two days on* 0.5 µg*/ml* α*CD3*ε *and* 1 µg*/ml* α*CD28 coated plates. On day 3 cells were removed from the stimulus, washed and expanded for a further 5 days. At day 7 post in vitro stimulation 6 million cells per sample were frozen as "day 7" activated cells. RNA from matched day 0 and day 7 samples was extracted on the same days.* ***B*** *The percentage of CD8 positive cells was determined by flow cytometry on the same day as cell pellets were frozen for RNA extraction.* ***C*** *A representative bioanlayser gel showing the typical banding pattern for a high quality RNA sample. The two prominent bands correspond to the 28S and 18S ribosomal RNA.* ***D*** *The bioanalyser electrophoretic trace corresponding to sample 79 day 7 shown in C. The trace is used to derive the RIN number.* ***E*** *RIN numbers for all samples included in the RNA-seq experiment as determined by the bioanalyser.*

4.2.2 Read mapping, fragment count and quality control

The subsequent bioinformatic analysis steps were performed with Martin Del Castillo Velasco-Herrera (PhD student in David Adams' team) following a previously published workflow (Anders et al., 2013). Reads were aligned to the reference genome (version GRCm38) using the splice-aware mapper tool STAR (Dobin et al., 2013) guided by version 84 of the Ensembl mouse annotation. Next, the number of read pairs (fragments) that uniquely aligned to a particular region in the genome were counted using Htseq-count (Anders et al., 2015). Between 21,786,497 and 49,939,333 reads were mapped per sample, 85.84 - 88.71% of which mapped uniquely to the reference genome. In order to estimate transcript expression levels, read counts were normalised by calculating the FPKM (see chapter 2, section 2.7) (Garber et al., 2011). Pairwise comparisons were performed with the log2-transformed FPKM values by calculating the pearson correlation coefficient of all possible comparisons. Hierarchical clustering showed that the samples clustered together according to which group (i.e. day 0 or day 7) they belonged to (Figure 4.2A), indicating that the gene expression differs between these two states of cells.

To further identify sources of variance in my dataset a PCA was performed (see chapter 2, section 2.7). In PCA, data points are projected onto a 2D plane. The x-axis represents the first principal component (PC1), which explains the greatest variance in the dataset. The y-axis represents the second principal component (PC2), which is independent from PC1 (Figure

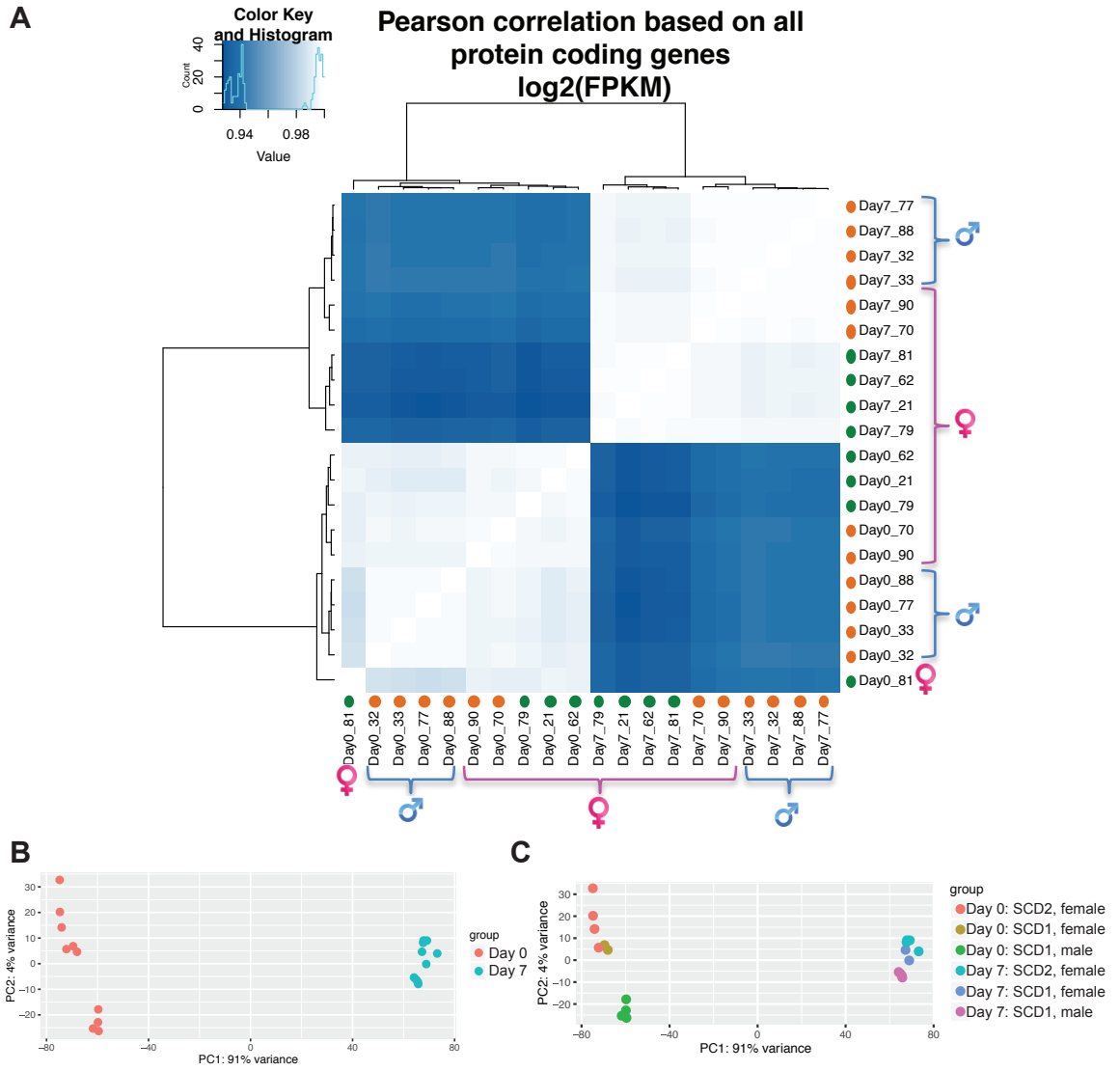

Fig. 4.2 ***RNA-seq quality control.***

Fig. 4.2 ***RNA-seq quality control.*** *RNA-seq was performed on RNA from CD8 T cells derived from 10 WT mice (4 males, 6 females) before stimulation and 7 days after stimulation.* ***A*** *Heatmap comparing samples pairwise in terms of the log2(FPKM) of all protein coding genes. White indicates a higher pearson correlation coefficient (samples on x and y axis are similar to one another), blue indicates a lower pearson correlation coefficient (samples on x and y axis are comparatively different from one another). The hierarchical clustering of the samples, as shown by the dendrogram, separates the samples by whether they belong to the day 0 group or the day 7 group. Samples were derived from ∼16 week old male or female mice and collected on two different spleen collection dates (SCD, orange = SCD 1, green = SCD 2) as indicated.* ***B*** *PCA was performed using the top 2000 most variable transcripts with regularised log transformed expression values for each sample. The percent of the total variance associated with each principal component is printed on the axis label. Samples are colour coded according to which group they belong to.* ***C*** *PCA plot where samples are colour coded according to which group they belong to, as well as which date the spleen was collected on and whether the spleen was derived from a female or male mouse. The plots in this figure were prepared with the help of Martin Del Castillo Velasco-Herrera. PC = principal component. SCD = spleen collection date.*

4.2B,C). In agreement with the data in Figure 4.2A, colour coding the samples showed that the group (i.e. whether a sample belongs to the group day 0 or day 7) is the biggest source of variance in my dataset. Expanding the colour code to include details such as spleen collection date and whether the samples were derived from males or females showed that samples also clustered together due to these factors. This demonstrated that all these factors affected gene expression, meaning that the spleen collection date should be accounted for in subsequent analyses.

4.2.3 Comparing gene expression in activated and naive CD8 T cells

The DESeq2 package (Love et al., 2014) was used to identify differentially expressed genes. DESeq2 tests for differential expression using a negative binomial distribution model (Anders and Huber, 2010). The spleen collection date was included as a covariate to accommodate this as a potential confounding factor. P-values were corrected for multiple testing using the Benjamini-Hochberg correction, giving an adjusted p-value (padj) (see chapter 2, section 2.7). In order to focus on genes with big changes in expression, genes were only considered

Table 4.1 ***Top 10 activated differentially expressed genes when comparing day 7 T cells to day 0 T cells.***

Gene	Log2(FoldChange)	p-value	B-H adjusted p-value
Spp1	11.793	0.00E+00	0.00E+00
Lif	10.579	0.00E+00	0.00E+00
Lrrc32	9.477	0.00E+00	0.00E+00
Gzmb	9.103	0.00E+00	0.00E+00
Cdkn1a	9.072	0.00E+00	0.00E+00
Tubb6	8.654	0.00E+00	0.00E+00
Il2ra	7.490	0.00E+00	0.00E+00
Galnt3	7.407	0.00E+00	0.00E+00
Slc16a3	7.397	0.00E+00	0.00E+00
Adam8	7.214	0.00E+00	0.00E+00

to be differentially expressed when the padj was smaller than 0.01 and the log2(fold change) was larger than 2 (upregulated genes) or smaller than -2 (downregulated genes).

The volcano plot in Figure 4.3A gives an overview of the number of differentially expressed genes. The fact that there were many significantly up and down regulated genes upon activation demonstrated how large the effect of activation is on the transcriptome of CD8 T cells. Genes that are highlighted in blue were detected as differentially expressed at 1% false discovery rate (FDR) and passed the log2(fold change) cut off. In total, there were 1803 activated and 2584 repressed significantly differentially expressed genes when comparing day 7 to day 0. From here on I will focus on the upregulated differentially expressed genes when comparing day 7 to day 0 samples, as this dataset should include the genes required for CTL effector functions. The top 10 upregulated genes, as ordered by the log2(fold change), are shown in Table 4.1. These included *Gzmb* and *Il2ra*, which encode granzyme B and the α-subunit of the high affinity IL2 receptor, respectively. These two proteins are known to be important for effector CTL function (de la Roche et al., 2016; Zhang and Bevan, 2011). The complete list of the 1803 upregulated differentially expressed genes is included digitally on a CD alongside this thesis (Appendix B).

To gain a better overall understanding of what biological pathways are enriched in the upregulated gene list, I used the Functional Interpretation of Differential Expression Analysis (FIDEA) server (D'Andrea et al., 2013). FIDEA mapped the genes in my dataset to functional categories in publicly available databases, such as Gene ontology (GO) (Gene Ontology Consortium et al., 2012) categories and Kyoto Encyclopaedia of Genes and Genomes (KEGG)

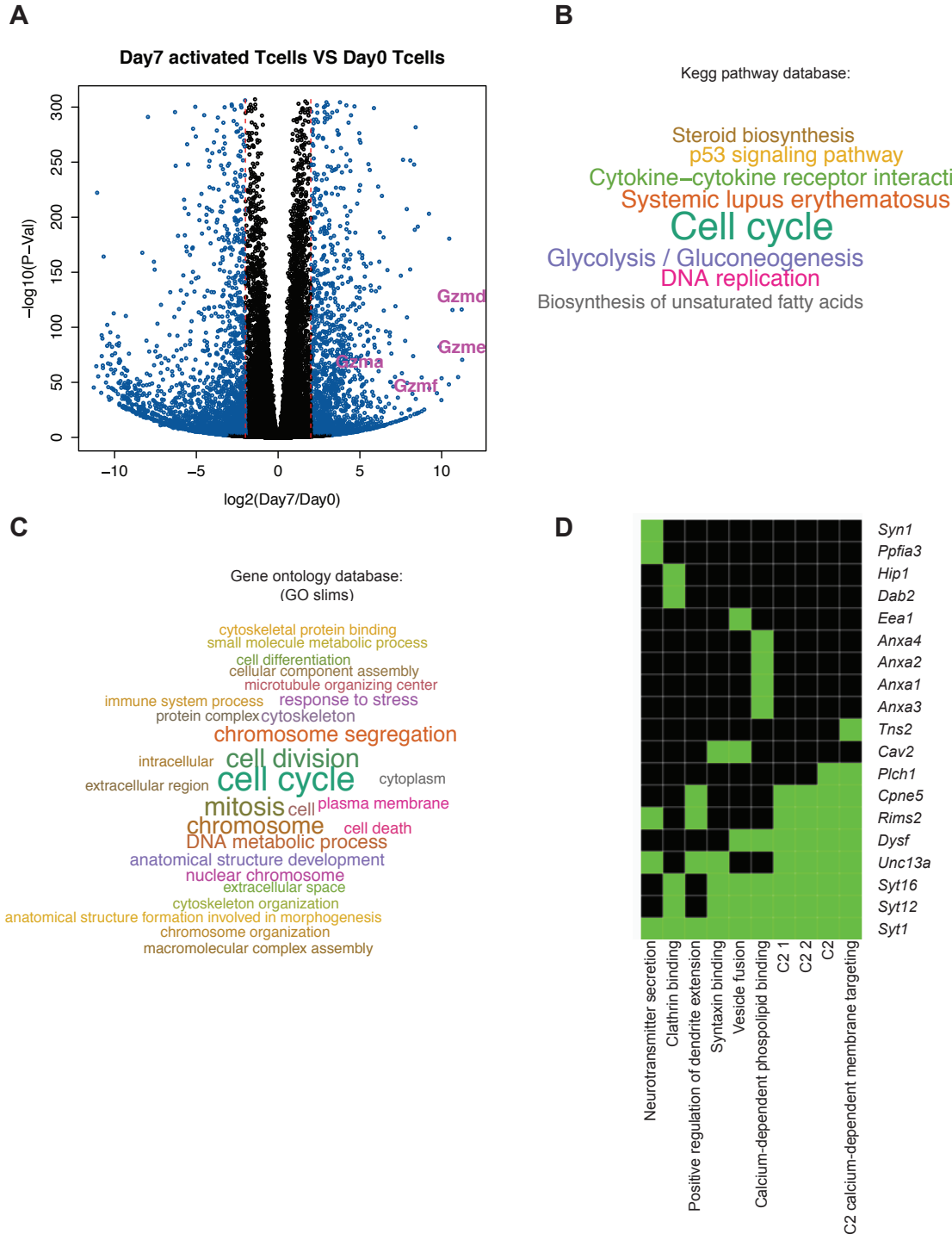

Fig. 4.3 ***Differential expression analysis between activated and naive CD8 T cells.***

Fig. 4.3 ***Differential expression analysis between activated and naive CD8 T cells.*** ***A*** *Volcano plot showing the -log10 of the p-value (y-axis) vs the log2 of the fold change of expression (x-axis) for each gene. Dotted lines indicate the log2(fold change) cut off at -2 and + 2. The blue colour is used to highlight genes that passed the log2(fold change) cut off and were detected as differentially expressed at 1% FDR when using the Benjamini-Hochberg multiple testing adjustment. Some genes encoding members of the granzyme protein family (Gzmd, Gzme, Gzmf and Gzma) are highlighted on the plot.* ***B*** *Word cloud derived from FIDEA mapping the significantly upregulated gene set to the KEGG pathway database. Words are sized according to enrichment using the FIDEA calculated p-value corrected for multiple testing.* ***C*** *Word cloud derived from FIDEA mapping the significantly upregulated gene set to the GO database. Words are sized according to enrichment using the FIDEA calculated p-value corrected for multiple testing.* ***D*** *Annotation cluster derived from the DAVID functional annotation tool that includes terms related to vesicle fusion, which could be relevant to CTL function. The heatmap shows the overlap between genes in my upregulated dataset (y-axis) and genes in the annotation cluster terms (x-axis). Green colour indicates that a gene is contained within the term, black colour indicates that a gene is not found in the term. FIDEA = Functional Interpretation of Differential Expression Analysis, DAVID = Database for Annotation, Visualization and Integrated Discovery, KEGG = Kyoto Encyclopaedia of Genes and Genomes, GO = Gene ontology.*

pathways (Kanehisa et al., 2012). These provide curated gene sets classified according to participation in common biological processes and can therefore be used to identify enriched biological themes in large gene lists. The gene sets are largely manually curated based on available experimental evidence and are therefore limited to published scientific knowledge (Gene Ontology Consortium et al., 2012). As each database has its own methods for assigning genes to categories it can be useful to compare the results obtained from separate curations. The results of the FIDEA analysis using KEGG and GO Slim databases are represented in word clouds (Figure 4.3B,C). The GO Slim database contains a smaller subset of the GO terms and is useful for broadly classifying which biological processes a set of genes is associated with (Gene Ontology Consortium, 2012). The size of the writing for each functional category in the word clouds corresponds to how enriched the particular category is in my dataset (D'Andrea et al., 2013). The word clouds particularly showed an enrichment of genes belonging to the "cell cycle" term of GO Slim and KEGG databases (Figure 4.3B,C). Other enriched pathways were pathways that are needed to replicate and make bigger cells, such as DNA replication and metabolism-related pathways (Figure 4.3B,C).

Using a different functional annotation tool, the Database for Annotation, Visualization and Integrated Discovery (DAVID) version 6.8 (Huang et al., 2009a,b) for functional enrichment analysis revealed 192 annotation clusters, representing biological processes, as enriched in the protein coding genes in my dataset. Annotation clusters group functionally similar terms together, with each term containing a list of genes associated with the term. DAVID determined whether these clusters were statistically overrepresented (enriched) in my dataset of upregulated genes. As for FIDEA, the sources of the functional annotation are databases such as KEGG and GO. One of the enriched clusters included terms related to vesicle fusion, which is a key event for CTL killing via the degranulation pathway (Dieckmann et al., 2016). The heatmap in Figure 4.3D visualises the overlap between upregulated genes in my dataset and the gene lists in the vesicle fusion annotation cluster. Ten genes were chosen from this list to target using CRISPR. These genes were *Ppfia3*, *Anxa1*, *Anxa2*, *Anxa3*, *Anxa4*, *Tns2*, *Cav2*, *Cpne5*, *Dysf* and *Unc13a*. Additionally, three other genes, *Slc7a5*, *Hif1*α and *Nfil3*, that were significantly upregulated in my activated gene list were added as further CRISPR targets. These three genes were previously found to have interesting phenotypes in CD8 T cells. Lack of SLC7A5 protein was shown to result in failure of CD8 T cells to differentiate into CTL (Sinclair et al., 2013) and HIF-1α and NFIL3, also known as E4BP4, depleted CD8 T cells were shown to lack perforin (Rollings et al., 2018). As these studies used mouse models, it would be interesting to test if these genes are also crucial for effector functions when only knocked out at day 4 post in vitro stimulation, as in my experimental set up. An overview of how differentially expressed the genes chosen for the targeted screen were can be seen in Table 4.2.

4.2.4 Targeted CRISPR screen

The genes of interest were targeted by CRISPR as explained in detail in chapter 3. In short, at day 4 post in vitro activation CTLs derived from OT-I mice were nucleofected with 3 crRNAs against the genes of interest, in addition to the tracrRNA reagent and Cas9 protein. Subsequently, CTLs were expanded for four days before measuring their degranulation and killing ability. As can be seen in Figure 4.4A, no degranulation defect was observed in response to targeting the genes of interest using CRISPR. Instead, some targets, most notably *Nfil3*, showed a trend towards increasing degranulation upon CRISPR treatment (Figure 4.4A). Two genetic targets, *Nfil3* and *Hif1*α, seemed to decrease CTL killing reproducibly after being targeted by CRISPR (Figure 4.4B).

Table 4.2 ***Differentially expressed genes chosen for the targeted CRISPR screen.***

Gene	Log2(FoldChange)	p-value	B-H adjusted p-value
Nfil3	5.450	0.00E+00	0.00E+00
Anxa2	4.143	0.00E+00	0.00E+00
Slc7a5	3.591	0.00E+00	0.00E+00
Hif1α	2.446	0.00E+00	0.00E+00
Unc13a	4.223	4.01E-202	1.19E-200
Anxa4	3.115	6.03E-191	1.60E-189
Anxa3	5.661	1.12E-138	1.82E-137
Anxa1	4.261	6.69E-117	8.39E-116
Cav2	5.133	5.14E-40	2.39E-39
Tns2	2.940	2.61E-27	9.64E-27
Cpne5	2.878	1.29E-20	4.16E-20
Ppfia3	2.963	4.34E-14	1.19E-13
Dysf	2.162	0.000626692	0.001118686

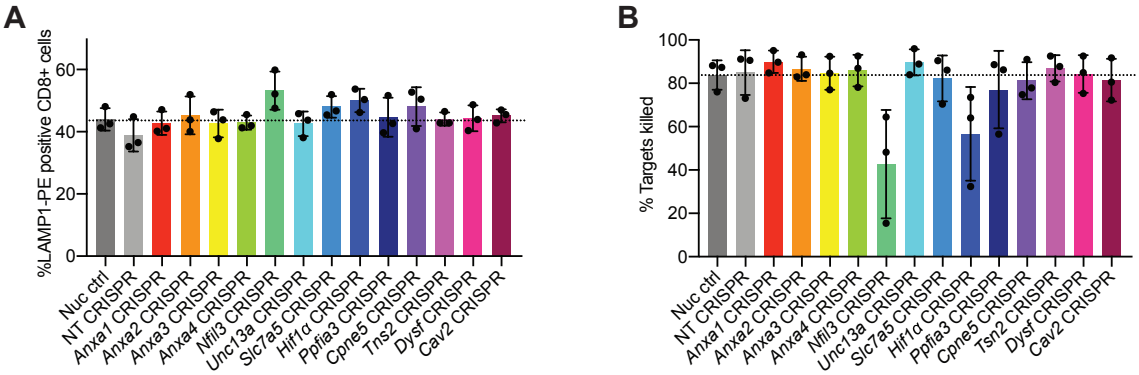

Fig. 4.4 ***Screening RNA-seq target genes using CRISPR.*** *CTLs were tested for their ability to degranulate and kill in response to exposure to EL4 target cells loaded with OVA-peptide.* ***A*** *The degranulation and* ***B*** *the killing readout of the combined degranulation and killing assays were analysed following the gating strategy and calculations described in chapter 2, section 2.5.1 and 2.5.2. E:T ratio = 2.5:1, assay duration = 180 min. The bar graphs show the average of 3 independent experiments, error bars show the SD. During each independent repeat the experiment was performed in technical duplicates.*

Based on the screening results, the effect of *Nfil3* and *Hif1α* CRISPR was investigated further. This confirmed that *Nfil3* CRISPR significantly increased degranulation (n=5, $p<0.05$, paired t-test) and decreased killing (n=5, $p<0.01$, paired t-test) as shown using two different killing assays (Figure 4.5A-C).

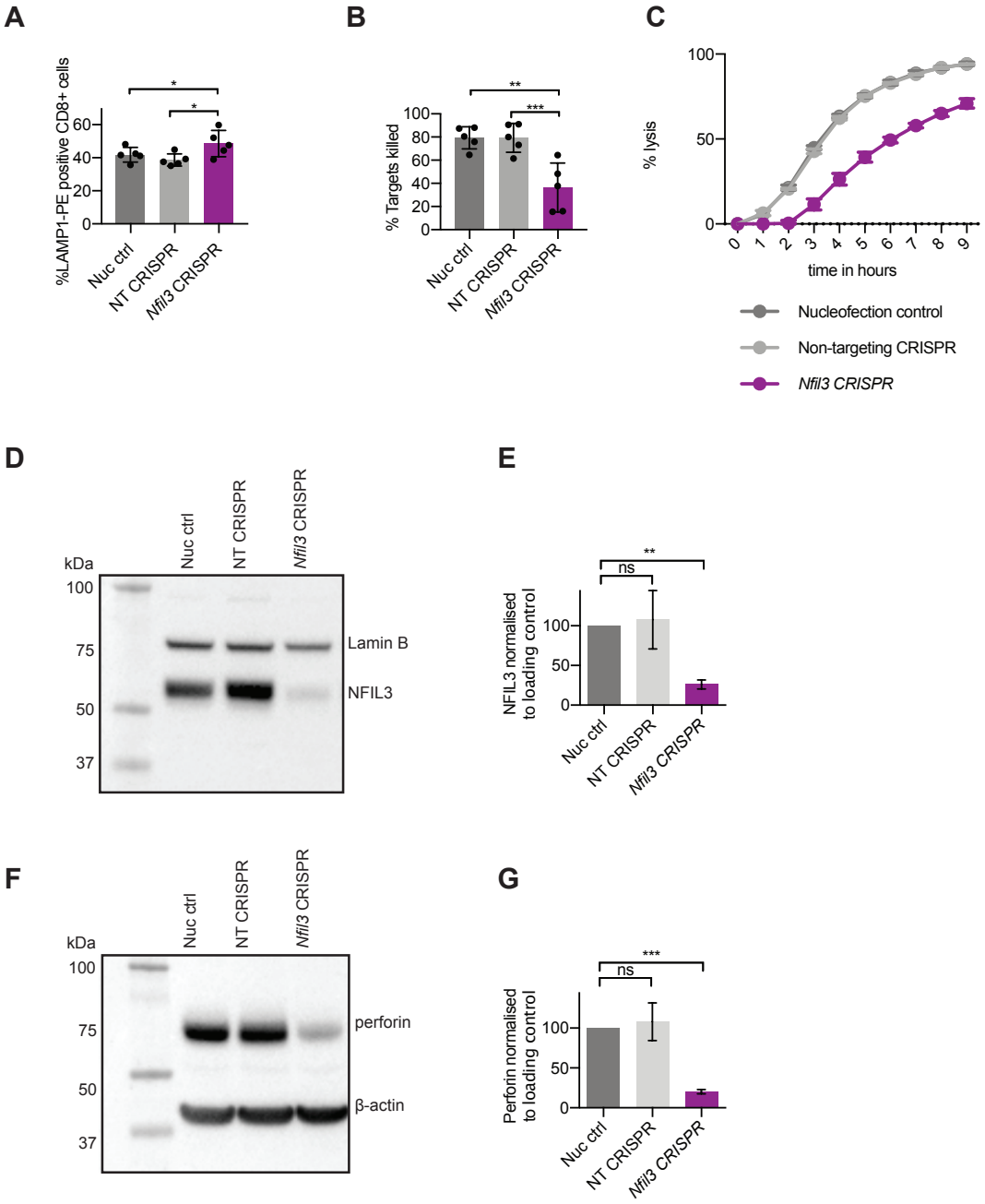

Fig. 4.5 ***Targeting Nfil3 by CRISPR resulted in a CTL killing defect.***

Fig. 4.5 ***Targeting Nfil3 by CRISPR resulted in a CTL killing defect.*** *OT-I CTL were nucleofected at day 4 after in vitro stimulation and tested in functional assays at day 8. CTLs were tested for their ability to degranulate and kill in response to exposure to EL4 target cells loaded with OVA-peptide.* ***A*** *The degranulation and* ***B*** *the killing readout of the combined degranulation and killing assays were analysed following the gating strategy and calculations described in chapter 2, section 2.5.1 and 2.5.2. E:T ratio = 2.5:1, assay duration = 180 min. The bar graphs show the average of 5 independent experiments, error bars show the SD. During each independent repeat the experiment was performed in technical duplicates, *p<0.05, **p<0.01, ***P<0.001 as calculated by paired t-test. Samples were paired by day of experiment to account for day-to-day fluctuations.* ***C*** *Incucyte killing assay readout showing % lysis of red EL4 target cells. One representative plot for 3 independent experiments is shown. E:T ratio = 10:1 Each datapoint corresponds to the mean ± SD of 3-4 technical repeats.* ***D*** *Representative WB showing NFIL3 and Lamin B1 (loading control) protein expression four days after nucleofection.* ***E*** *Quantification of the NFIL3 protein level. In each repeat the NFIL3 protein level was expressed relative to the nucleofection control and normalised to the loading control, n=3 independent experiments, **p<0.01 calculated by one-sample t-test.* ***F*** *Representative WB showing perforin and β-actin (loading control) protein expression four days after nucleofection.* ***G*** *Quantification of the perforin protein level. In each repeat the perforin protein level was expressed relative to the nucleofection control and normalised to the loading control, n=3 independent experiments, ns = not significant, ***p<0.001 calculated by one sample t-test. All bar graphs show the mean ± SD.*

Hif1α CRISPR also significantly decreased the ability of CTLs to kill (n=5, p<0.01, paired t-test), but only showed a trend towards increasing degranulation (Figure 4.6A-C). To validate CRISPR efficiency I tested for target protein expression by WB. Decreased NFIL3 protein levels were observed in *Nfil3* CRISPR samples (n=3, p<0.01, one sample t-test) (Figure 4.5D,E). HIF-1α protein could initially not be detected by WB, most likely because the samples were unstimulated and kept under normoxic conditions (Nakamura et al., 2005). When stimulated with αCD3ε for 4 h in hypoxic conditions (1% O_2) HIF-1α could be detected by WB, and HIF-1α levels were found to be reduced in *Hif1α* CRISPR samples (n=1) (Figure 4.6D). Additionally, *Hif1α* CRISPR samples were shown to have decreased NFIL3 protein levels (n=2) (Figure 4.6E,F), which was in agreement with a study where *Hif1α* was deleted in all Vav-expressing cells using the Cre-lox system in mice (Rollings et al., 2018).

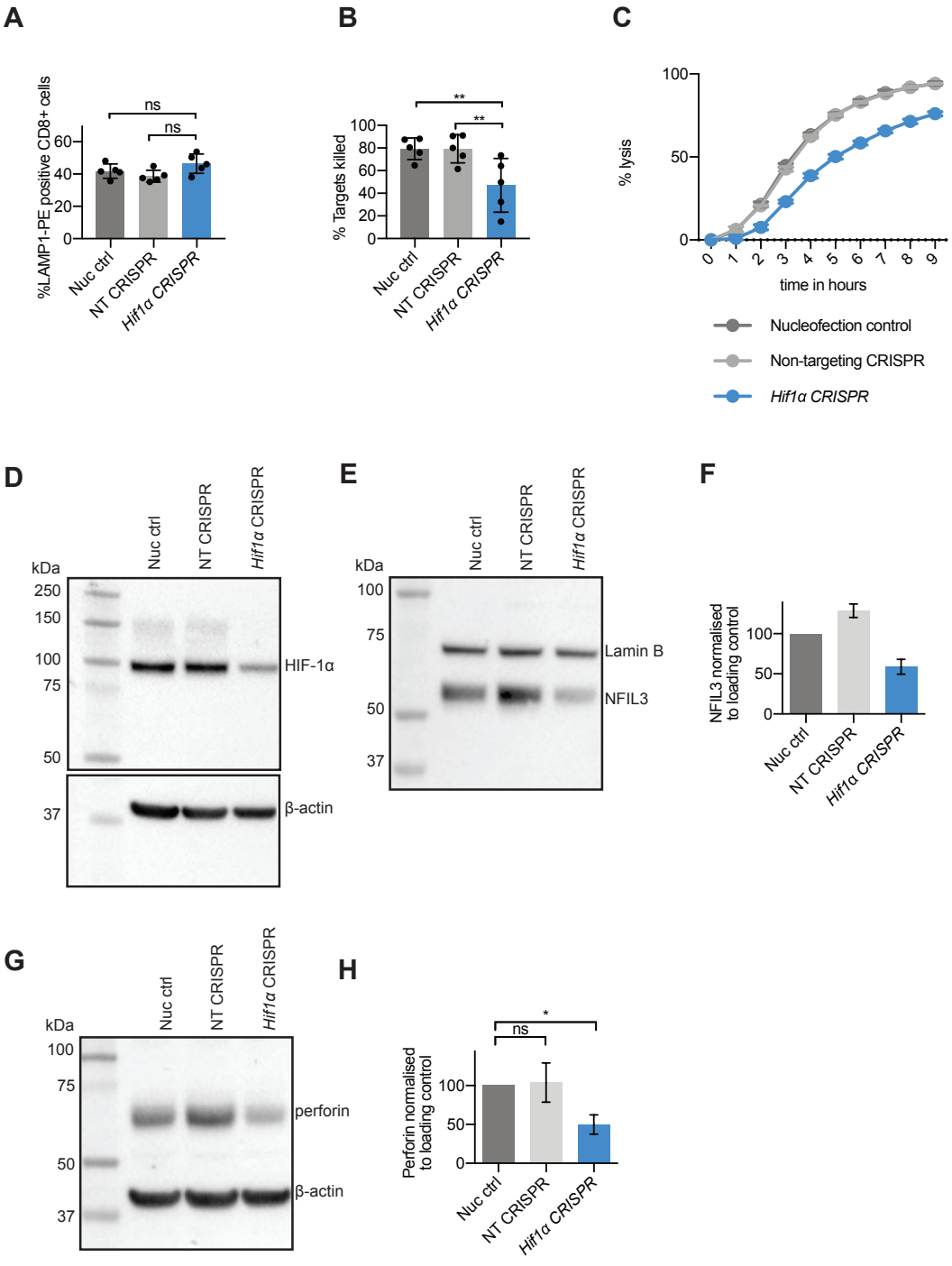

Fig. 4.6 ***Decreased killing in response to targeting Hif1α by CRISPR.***

Fig. 4.6 ***Decreased killing in response to targeting Hif1α by CRISPR.*** *OT-I CTL were nucleofected at day 4 after in vitro stimulation and tested in functional assays at day 8. CTLs were tested for their ability to degranulate and kill in response to exposure to EL4 target cells loaded with OVA-peptide.* ***A*** *The degranulation and* ***B*** *the killing readout of the combined degranulation and killing assays were analysed following the gating strategy and calculations described in chapter 2, section 2.5.1 and 2.5.2. E:T ratio = 2.5:1, assay duration = 180 min. The bar graphs show the average of 5 independent experiments, error bars show the SD. During each independent repeat the experiment was performed in technical duplicates, **p<0.01 as calculated by paired t-test. Samples were paired by day of experiment to account for day-to-day fluctuations.* ***C*** *Incucyte killing assay readout showing % lysis of red EL4 target cells. One representative plot for 3 independent experiments is shown. E:T ratio = 10:1 Each datapoint corresponds to the mean ± SD of 3-4 technical repeats.* ***D*** *WB showing HIF-1α and β-actin (loading control) protein expression four days after nucleofection of CRISPR reagents and 4 h after αCD3ε stimulation under hypoxic conditions, n=1.* ***E*** *Representative WB showing NFIL3 and Lamin B1 (loading control) protein expression four days after nucleofection.* ***F*** *Quantification of the NFIL3 protein level. In each repeat the NFIL3 protein level was expressed relative to the nucleofection control and normalised to the loading control, n=2 independent experiments.* ***G*** *Representative WB showing perforin and β-actin (loading control) protein expression four days after nucleofection.* ***H*** *Quantification of the perforin protein level. In each repeat the perforin protein level was expressed relative to the nucleofection control and normalised to the loading control, n=3 independent experiments, ns = not significant, *p<0.05 calculated by one sample t-test. All bar graphs show the mean ± SD.*

The phenotype of increased degranulation and decreased killing was reminiscent of the phenotype observed upon *perforin* CRISPR (Figure 3.8). Other studies showed that deleting components of the HIF-1 complex or NFIL3 in mice resulted in decreased perforin expression (Finlay et al., 2012; Rollings et al., 2018). I therefore investigated the effect of *Hif1α* and *Nfil3* CRISPR on perforin protein levels by WB, which confirmed that perforin was decreased in *Hif1α* (n=3, p<0.05, one sample t-test) and *Nfil3* CRISPR samples (n=3, p<0.001, one sample t-test) (Figure 4.5F,G and Figure 4.6G,H).

4.2.5 Comparing gene expression in activated CD8 T cells derived from males and females

As the PCA plot in Figure 4.2 indicated that some of the variance in my dataset was due to differences between sexes, I investigated which genes were differentially expressed between CD8 T cells derived from males and females. For this, I compared male and female samples derived from the day 7 group and applied the same significance thresholds as before to identify differentially expressed genes (padj<0.01, log2(fold change) >2 or <-2). Differentially expressed genes that passed these stringent selection criteria were limited to *Ddx3y*, *Kdm5d*, *Eif2s3y* and *Uty*, all of which are located on the Y chromosome according to the NCBI website (Table 4.3). Not taking into account the stringent log2(fold change) cut-off revealed 79 significantly up- or down regulated genes (all with padj<0.01). Interestingly, this gene list included *Nfil3*, as well as genes that encode several different granzymes (Table 4.3).

Table 4.3 ***Differentially expressed genes when comparing activated T cells derived from males to activated T cells derived from females.***

Gene	Log2(FoldChange)	p-value	B-H adjusted p-value
Ddx3y	4.231	0.00E+00	0.00E+00
Kdm5d	3.348	0.00E+00	0.00E+00
Eif2s3y	3.081	0.00E+00	0.00E+00
Uty	2.478	1.18E-206	4.07E-203
Eif2s3x	-0.649	7.24E-29	2.00E-25
Kdm5c	-0.481	2.10E-23	4.81E-20
Kdm6a	-0.627	1.85E-22	3.64E-19
Il10	-0.651	1.93E-17	3.32E-14
Pbdc1	-0.477	6.07E-14	9.29E-11
Gm29650	0.333	3.93E-13	5.41E-10
Fosb	-0.519	3.29E-11	4.12E-08
Gldc	0.379	8.06E-11	9.25E-08
Esm1	-0.414	5.19E-10	5.49E-07
Eng	-0.488	1.24E-09	1.22E-06
Gm5861	-0.471	1.37E-09	1.26E-06
Cdh17	-0.456	1.10E-08	9.46E-06
Gzma	-0.377	1.47E-08	1.16E-05
Tcrg-C2	-0.447	1.51E-08	1.16E-05
Maf	0.425	3.14E-08	2.17E-05

Table 4.3 continued from previous page

Gene	Log2(FoldChange)	p-value	B-H adjusted p-value
Gzmf	-0.39	3.13E-08	2.17E-05
5530601H04Rik	-0.424	3.69E-08	2.31E-05
Epas1	-0.426	3.59E-08	2.31E-05
Xist	-0.211	8.06E-08	4.82E-05
Pkhd1l1	-0.388	1.41E-07	8.11E-05
Gzmc	-0.384	2.63E-07	0.000145102
Cyp11a1	-0.248	3.82E-07	0.000202287
Pparg	-0.297	4.70E-07	0.000239877
Epsti1	0.282	6.22E-07	0.000295237
Gm8897	-0.373	6.17E-07	0.000295237
Ms4a4c	0.37	8.01E-07	0.000367891
Csgalnact1	-0.304	9.44E-07	0.000406428
Slc16a10	-0.395	9.19E-07	0.000406428
She	0.334	9.76E-07	0.000407425
Batf3	-0.332	1.01E-06	0.000407867
Cxcr6	0.381	1.08E-06	0.000411676
Btla	0.378	1.08E-06	0.000411676
Spry2	-0.385	1.70E-06	0.000632598
Il24	-0.293	2.09E-06	0.000757181
Speer1	-0.337	2.29E-06	0.000809682
Nfil3	-0.299	3.90E-06	0.001343211
Procr	-0.266	4.08E-06	0.001369305
Scin	-0.307	6.21E-06	0.002035039
Fcgrt	0.271	7.35E-06	0.002355526
Avil	-0.353	7.72E-06	0.002416567
Trp53inp1	0.335	8.60E-06	0.002576152
Prss12	0.317	8.56E-06	0.002576152
Map1a	0.324	8.92E-06	0.002613249
Arhgap4	0.212	9.15E-06	0.002625824
Mxd4	0.343	9.63E-06	0.002678748
Mcpt8	-0.27	9.72E-06	0.002678748
Spire1	-0.292	1.21E-05	0.003170046
Gm8890	-0.3	1.22E-05	0.003170046

Table 4.3 continued from previous page

Gene	Log2(FoldChange)	p-value	B-H adjusted p-value
Atf3	-0.349	1.20E-05	0.003170046
Jdp2	-0.327	1.39E-05	0.0035429
Gm19705	0.341	1.57E-05	0.003862068
Gm8879	-0.299	1.57E-05	0.003862068
Il6ra	0.28	1.72E-05	0.00402067
Loxl2	-0.244	1.71E-05	0.00402067
Gzmg	-0.265	1.67E-05	0.00402067
Cd7	0.285	1.90E-05	0.004372669
Trgv2	-0.341	1.95E-05	0.004401909
Il2ra	-0.222	2.21E-05	0.004918823
Cxcr3	0.326	2.35E-05	0.005068284
Pisd-ps1	-0.291	2.35E-05	0.005068284
Fkbp11	-0.285	2.43E-05	0.005098991
Lag3	-0.339	2.44E-05	0.005098991
Epdr1	-0.238	2.61E-05	0.005361774
Fcer1g	-0.331	2.76E-05	0.005581624
Vipr1	0.297	3.16E-05	0.006255572
Tcrg-C4	-0.327	3.18E-05	0.006255572
Dgka	0.264	3.31E-05	0.006429906
Myo1e	-0.314	3.68E-05	0.007031746
Nt5e	0.331	3.84E-05	0.007150566
Plcg2	-0.267	3.81E-05	0.007150566
Nod1	0.292	4.79E-05	0.008801724
Tmem37	0.319	4.98E-05	0.00902281
Slc22a21	-0.247	5.06E-05	0.00905477
Chd3	0.263	5.66E-05	0.009986283
Slc4a7	-0.3	5.73E-05	0.009986283

4.3 Discussion

The RNA-seq study set up was designed to show differences between the transcriptome of naive CD8 T cells and effector CD8 T cells that were stimulated and kept in culture for 7 days (Figure 4.1A). The heatmap and PCA plots in Figure 4.2 demonstrated that samples

were mainly separated according to whether the RNA was derived from naive cells (day 0) or effector cells (day 7), indicating that the gene expression differs between these two states of cells. The PCA plots further revealed that some variance in the dataset was due to the spleen collection date and whether samples were derived from males or females (Figure 4.2C). The former was accounted for during subsequent analysis steps.

Differential expression analysis using the DESeq2 package revealed 1803 differentially expressed genes where gene expression is upregulated, and 2584 differentially expressed genes where gene expression is downregulated. Subsequently, I focussed on the 1803 activated differentially expressed genes, as this dataset should include genes that are required for CTL killing. However, this dataset will additionally also include genes that are required for other processes in T cell differentiation to cytolytic effectors, such as cell proliferation and switching glucose metabolism from oxidative phosphorylation to glycolysis to fuel cell growth (Fox et al., 2005). Using the functional annotation tool FIDEA confirmed that most of the genes in my activated dataset associated with pathways related to proliferation (e.g. cell cycle) (Figure 4.3B,C). This was reproducible using two different curations, KEGG and GO, for the analysis (Figure 4.3B,C).

While I could have taken the approach to target the top upregulated genes in my dataset (Table 4.1), a more targeted approach to isolate genes that may affect CTL killing was chosen instead due to the concerns mentioned above. The DAVID functional annotation tool was used in order to identify annotation clusters of genes related to what is known to be important for CTL killing function. An annotation cluster was identified that was enriched in my dataset and contained gene lists associated with vesicle fusion (Figure 4.3D). Vesicle fusion is known to be important during the degranulation mechanism of CTL killing. 10 genes were chosen from this list with a focus on genes that had not been studied extensively in CTL. Additionally, 3 other genes were included that were identified as interesting targets from the literature (Finlay et al., 2012; Rollings et al., 2018; Sinclair et al., 2013).

The screen was performed in primary mouse CTL derived from OT-I mice as these had been used successfully with the CRISPR technology (chapter 3) and were readily available in the Griffiths lab. The results of the RNA-seq study should be applicable to the OT-I system, as these mice are bred on a C57BL/6 background. T cells derived from OT-I mice express the OT-I TCR, which specifically recognises the OVA peptide presented by the H-2K^b MHC class I molecule (Hogquist et al., 1994). Out of the 13 genes that were targeted by CRISPR (Table 4.2), only *Hif1*α and *Nfil3* showed a reproducible phenotype across three independent

repeats (Figure 4.4). Due to time constraints, the other 11 genes were not followed up further. However, I can not conclude that these genes have no effect on CTL degranulation or killing without validating that the genes were successfully targeted by CRISPR. Since not all of these genes have commercially available antibodies against their protein, the effect of CRISPR could instead be confirmed by sequencing the DNA or by looking at the mRNA levels using qRT-PCR. While these techniques would show if a cut occurred at the DNA level, or if there is a decrease in mRNA, respectively, neither approach would be guaranteed to reflect the expression of functional protein.

The killing defect observed in response to *Nfil3* and *Hif1α* CRISPR was confirmed using two different in vitro killing assays (Figure 4.5B,C and Figure 4.6B,C). Western blotting confirmed that NFIL3 protein levels were decreased upon *Nfil3* CRISPR (Figure 4.5D,E). HIF-1α protein levels were only detectable by WB after samples were stimulated with αCD3ε under hypoxic conditions (Figure 4.6D). Other studies have shown that while HIF-1α cannot be detected by WB when effector CTL are kept under normoxic conditions, HIF-1α levels are increased after switching cells to hypoxic conditions and in response to TCR stimulation (Doedens et al., 2013; Nakamura et al., 2005; Palazon et al., 2017; Rollings et al., 2018). In agreement with the literature, NFIL3 levels were reduced in *Hif1α* CRISPR samples, providing further evidence that the *Hif1α* gene was successfully targeted by CRISPR (Figure 4.6E,F). Furthermore, perforin protein levels were decreased in both *Nfil3* and *Hif1α* CRISPR samples (Figure 4.5F,G and Figure 4.6G,H). This has previously been observed in a study using the Cre-lox system, with Cre expression under the control of the *vav*-promoter, to delete *Nfil3* and *Hif1α* in hematopoietic cells (Rollings et al., 2018). However, HIF-1 regulation of perforin was found to be indirect, as the perforin promoter did not contain HIF-1 complex binding sites (Finlay et al., 2012). In future experiments, it would be interesting to investigate whether the *Nfil3* promoter contains HIF-1α binding sites, to determine whether *Nfil3* is directly regulated by HIF-1α. Additionally, it would be interesting to overexpress NFIL3 in *Hif1α* KO cells. If this rescues the killing phenotype it could suggest that the killing defect in *Hif1α* KO CTLs is mediated via NFIL3.

Although the exact mechanism by which *Hif1α* and *Nfil3* KO lead to a decrease in perforin is not understood, this explained at least in part why targeting these genes by CRISPR resulted in a CTL killing defect at the molecular level. In agreement with my findings, other studies showed that deletion of the HIF-1 complex in CTL resulted in decreased production of other effector molecules (IFNγ, TNFα and granzyme B) as well as reduced tumour cell killing in vivo (Finlay et al., 2012; Palazon et al., 2017). Meanwhile, increased *Hif1α* expression,

achieved through the loss of one of the main negative regulators of the HIF transcription factors (the von Hippel-Lindau complex), resulted in increased effector function of CTL, as measured by an increase in the expression of effector molecules, such as granzyme B and perforin, and in an in vivo cytotoxicity assay (Doedens et al., 2013). Additionally, *Nfil3* KO mice were found to have severely reduced levels of peripheral NK cells and impaired NK cell cytotoxicity (Gascoyne et al., 2009).

In addition to comparing the transcriptome of effector and naive CD8 T cells, my RNA-seq dataset also allowed me to compare effector CD8 T cells derived from male and female mice. Only Y-linked genes passed the log2(fold change)>2 or <-2 and padj<0.01 cut offs (Table 4.3). This was expected, as females do not have Y chromosomes. Looking at the genes that were significantly differentially expressed (padj<0.01), but had a smaller effect size (log2(fold change)>-2 and <2), interestingly identified that CD8 T cells derived from males had less mRNA encoding several members of the granzyme family, IL2RA and NFIL3 (Table 4.3). It would therefore be interesting to compare expression of NFIL3 protein between males and females, to see if this transcriptional effect is also present at the protein level. Furthermore, it could be investigated whether this also translates to a better killing capability in cells derived from female mice.

In summary, my data, together with published studies, convincingly showed that HIF-1α and NFIL3 are crucial for CTL killing function. The data in this chapter demonstrated that loss of NFIL3 and HIF-1α showed an effect even when these genes are only knocked out in effector CTL. This indicated that the phenotype is not dependent on HIF-1α and NFIL3 being absent during T cell development or effector CTL differentiation. Furthermore, the RNA-seq dataset revealed interesting differences in expression of mRNAs encoding NFIL3 and several cytotoxic effector molecules between CTLs derived from male and female mice.

4.3.1 Summary and evaluation of aims

- Determine the differences in gene expression between naive and activated CD8 T cells. The hypothesis is that there are substantial changes in gene expression between these two states of CD8 T cells.
  - Significant differences in gene expression were observed: 1803 significantly activated differentially expressed genes with padj<0.01 and log2(fold change)>2 were identified using DESeq2.

- Explore the functional association of the differentially expressed genes using bioinformatic tools.
  - Using FIDEA and DAVID bioinformatic tools identified that upregulated genes in my dataset predominantly associated with pathways related to cell proliferation, which was not unexpected as CD8 T cells undergo rapid clonal expansion upon stimulation.
- Test the effect of targeting differentially expressed genes by CRISPR in phenotypic assays (degranulation and killing assays).
  - *Hif1α* and *Nfil3* were identified as interesting genetic targets that decreased killing but not the degranulation capability of CTL. *Hif1α* and *Nfil3* have previously been identified as affecting CD8 T cell cytotoxicity in KO mouse models (Doedens et al., 2013; Finlay et al., 2012; Rollings et al., 2018). Here I show that loss of these genes also had an effect on cytotoxicity when expression of these genes is only lost in differentiated effector CTL in vitro, as opposed to in naive T cells or during T cell development in vivo. This suggested a more immediate importance of these genes in CTL killing.
- Explore what genes are differentially expressed in CD8 T cells derived from male and female mice.
  - Highly differentially expressed genes (log2(fold change)>2) were limited to Y-linked genes when comparing males to females. Interestingly, genes that were significantly differentially expressed, but that did not pass the stringent log2(fold change) cut-off, included genes known to be important for CTL function (such as *Gzma* and *Il2ra*), as well as *Nfil3*.

Chapter 3 and chapter 4 make up the portion of the thesis that focuses on primary mouse T cells. One of the main conclusions from this aspect of the PhD project is that gene expression in primary mouse CTLs can be efficiently disrupted using the CRISPR Cas9-RNP approach as optimised in the last two chapters. Importantly, this approach can be used in cells derived from any mouse line, regardless of the genetic background. This provides an effective and versatile tool to study the function of genes in primary mouse T cells.

Additionally, the newly established assay that simultaneously measures degranulation and killing can be used to identify phenotypes of interest, as demonstrated using an arrayed CRISPR screen. The readout of the assay was reliable, as comparable results were obtained

using a separate phenotypic assay, the Incucyte killing assay. In combination with the optimised CRISPR technology, the assay enables to identify genes important for CTL killing and/or degranulation.

In hindsight, the experimental design of the RNA-seq study could have been more targeted to the overall aim of the thesis, which was to identify regulators of CTL killing. Instead, the RNA-seq study more broadly identified genes that are implicated in CD8 T cell activation. While some of the genes upregulated in response to activation are necessary for CTL killing, they are overshadowed by genes important for other biological functions, such as the proliferation response. A possible alternative approach would have been to incorporate purified CD4 T cells in the study design. Comparing the transcriptome of activated CD4 and CD8 T cells would have allowed to filter out genes associated with proliferation in response to activation, and would have revealed genes relevant for CD8 T cell specific functions. Nonetheless, the RNA-seq dataset presented in this chapter is a useful resource, as it presents a comprehensive readout of all genes that are expressed in primary mouse naive and activated CD8 T cells.